IEEE Access
Multidisciplinary ⋮ Rapid Review ⋮ Open Access Journal

Received December 6, 2020, accepted January 8, 2021, date of publication January 13, 2021, date of current version January 22, 2021.

Digital Object Identifier 10.1109/ACCESS.2021.3051404

UKF-Based Sensor Fusion Method for Position Estimation of a 2-DOF Rope Driven Robot

MYEONGJIN CHOI[1], MYOUNGJAE SEO[1], HWA SOO KIM[2], (Member, IEEE), AND TAEWON SEO[1], (Senior Member, IEEE)

[1]School of Mechanical Engineering, Hanyang University, Seoul 04763, South Korea
[2]Department of Mechanical System Engineering, Kyonggi University at Suwon, Suwon 16227, South Korea

Corresponding authors: Taewon Seo (taewonseo@hanyang.ac.kr) and Hwa Soo Kim (hskim94@kgu.ac.kr)

This work was supported by the National Research Foundation of Korea (NRF) Grant funded by the Ministry of Science and ICT for the First-Mover Program for Accelerating Disruptive Technology Development under Grant 2018M3C1B9088331 and Grant 2018M3C1B9088332.

ABSTRACT In this study, the unscented Kalman filter-based method was introduced as a new technique for position estimation of the two-degree-of-freedom façade cleaning robot known as the Dual Ascender Robot (DAR). While other façade cleaning robots use a winch, the DAR uses an ascender, resulting in rope slip inside the ascender. Rope slip does easily cause errors in length data, so DARs cannot be easily controlled based on length data as in the case of most façade cleaning robots. Therefore, the DARs estimate the length data and use it through position estimation to overcome the rope slip for control. DARs use a rope length-based sensor fusion method for position estimation. This method employs position data based on both length data and angle data to estimate the position; however, it is difficult to use for long periods of time owing to the increased error that accumulates with time. Therefore, the use of position data based on angle data is proposed herein via application of the unscented Kalman filter. This unscented Kalman filter-based method is tested to confirm that the positional estimation performance is improved relative to that achieved via the previously used method. The performance improvements are compared in terms of accuracy and repeatability using the double ball bar method, and the errors in accuracy and repeatability are found to be reduced by approximately 2–3 times.

INDEX TERMS Dual ascender robot, façade cleaning robot, sensor fusion, unscented Kalman filter, position estimation, IMU sensor.

I. INTRODUCTION

Buildings of increased heights are being constructed to use space efficiently in cities. However, such increases in building heights prove disadvantageous from the perspective of building maintenance. For maintaining cleanliness in such a building, a person must hang on a rope to clean the building; however, this is dangerous because no safety measures can be provided in such a scenario. Therefore, research is being actively conducted in various fields to help reduce the risk borne by exterior wall cleaners. In this context, façade cleaning robots have been investigated in robot studies [1].

Most façade cleaning robots, such as building exterior wall cleaners, use ropes to move over walls. Therefore, the degrees of freedom (DOFs) and movement are determined by the number of ropes used by the robot. Façade cleaning robots using one rope include SkyPro [2], [3], IPC Eagle [4], [5], ROPE RIDE [6], and Tito 500 [7]. These possess one degree of freedom (DOF) to move upward and downward. Such 1-DOF movement is advantageous in terms of the simple control involved at varying speeds, regardless of the position of the robot. However, the disadvantage here is a longer cleaning time because the robot is not free to move around significantly. Façade cleaning robots having 2 or more DOFs and using two or more ropes are also being investigated to compensate for the disadvantages of 1-DOF façade cleaning robots. Such robots can move not only upward and downward but also in both sideward directions. KITE [8], SkyScraper-I [9], and the DAR [10] are typical examples of robots with more than 2-DOFs. Façade cleaning robots with more than 2-DOFs inevitably require control because they must exhibit movements in more than 2 DOFs using

The associate editor coordinating the review of this manuscript and approving it for publication was Rui-Jun Yan.

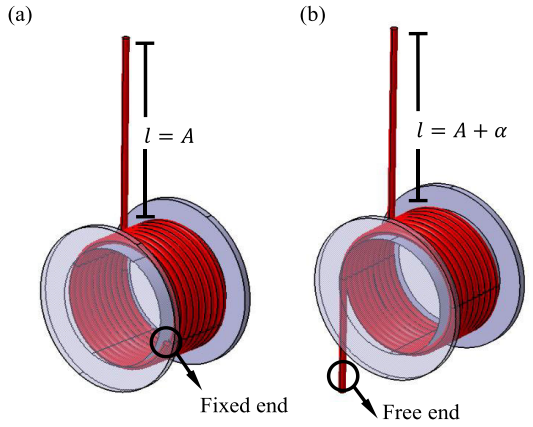

FIGURE 1. Difference between winch and ascender; (a) winch has a fixed end point, so the rope length can be measured as a single constant value; (b) ascender does not have a fixed end point, so the rope length measured may contain an error.

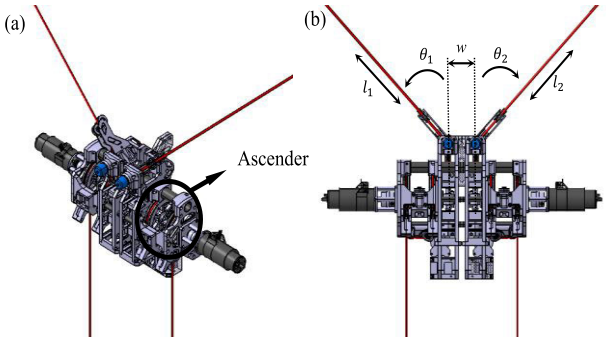

FIGURE 2. Actual appearance of dual ascender robot (DAR); (a) isometric view of DAR. Each rope is wound to the ascender; (b) front view of DAR. Rope length data, data of angle between rope and robot, and robot rotation angle are measured using several sensors.

rope alone. The control method used in such a case employs the rope length data. Façade cleaning robots with more than 2 DOFs using rope employ a mechanical device called a winch that winds and releases the rope; however, changes in the rope length are not caused because the end points are fixed when the robot is installed on the building, as shown in Fig. 1 (a). Therefore, the robots equipped with a winch consider this unchanged rope length data for modeling and control. However, among the façade cleaning robots that employ more than two ropes such as DAR cannot use the rope length data for control. Because the structural properties of the DAR do not require the use of a winch, the DAR exhibits 2-DOF movement on the outer wall of the building with a unique method of control.

The DAR possessing structural properties involving the use of such a unique method of control is shown in Fig. 2 (a). For each rope, the DAR uses a mechanical device called an ascender, which is similar to a winch. However, there is one difference between the ascender and winch. When the robot is installed on the building, there is no fixed end point of the rope inside the ascender. Therefore, each time the rope is wound and released inside the ascender, rope slip occurs and a change in the rope length is caused, as shown in Fig. 1 (b). This implies that the DAR cannot use the control method that most 2-DOF façade cleaning robots use.

To overcome rope slip inside the ascender, the DAR must use the position data of the robot. Rope length data have been previously obtained using inverse kinematics through the robot position data and used for control. Owing to this unique process, the DAR requires the correct robot position data; the process of determining the position for control of the DAR has therefore been defined as position estimation. The position estimation process employed by the DAR uses the various data that the robot comprises [11]. Fig. 2 (b) shows these data; l_i is the rope length, θ_i is the angle between the rope and the robot, and w is the distance between the rope joints. The data are combined using forward kinematics to create two-position data. The sensor fusion method is then employed to apply the two-position data to position estimation. However, error accumulates over time because the existing position estimation method considers the error rope length l_i for position estimation.

The rope angle-based Kalman filter method is proposed to improve the accuracy of positioning of the DAR [12]. This method involves the application of an unscented Kalman filter to the position data used in the previous position estimation method and sensor fusion method. In the sensor fusion method, a cumulative error in position estimation is obtained on using the error rope length; however, the rope angle-based Kalman filter method is suitable for use in DARs because it can capture the rope length error through filtering. For the purpose of obtaining a comparison across different scenarios, the same experiment was conducted to compare the position of the robot obtained via the previous sensor fusion method, and the new rope angle-based Kalman filter method.

The remainder of this paper is organized as follows. Section 2 presents more details regarding the DAR position estimation method previously used, and Section 3 discusses the proposed rope angle basesd Kalman filter method to be applied for improving the position estimation of the DAR. Section 4 describes an experiment used to compare the performance of the previous sensor fusion method with that of the Kalman filter method. Section 5 presents the verification of the experimental results and discusses whether the positioning ability is improved via application of the Kalman filter method to the DAR. Finally, in Section 6, the study is concluded through an evaluation of the new DAR position estimation method

II. PREVIOUS DAR'S POSITION ESTIMATION METHOD

In previous studies, DARs employed a unique rope length-based sensor fusion method to estimate the position [10]. This sensor fusion method used data received from various sensors on the robot to perform position estimation. The details of these sensors are summarized in Table 1. Through the angle of rotation of the rotary encoder on the rope end

TABLE 1. Specifications of DAR's sensors.

	Sensor type	Model	Producer	Resolution
Rope length (l_i)	Incremental encoder	E30S4-100-3-N-5	Autonics	0.16 mm
Rope angle (θ_i)	Incremental encoder	E30S4-3000-3-N-5	Autonics	0.04 °
Robot angle (ψ)	IMU sensor	EBIMU-9DOFV5	E2BOX	0.01 °

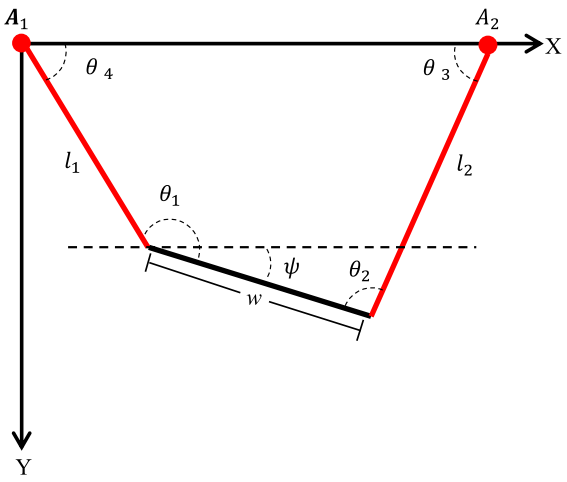

FIGURE 3. Dual ascender robot's modeling on global coordinate.

point, the angle data ($\boldsymbol{\theta_i}$) were obtained; through the degree of rotation of the pulley connected to the rotary encoder on the side, the length data ($\boldsymbol{l_i}$) were obtained; this length was increased and decreased. In the inertial measurement unit (IMU) sensor, the roll value was read to obtain the angle ψ, which is the angle the robot returned, as shown in Fig. 3. After the obtained data were fused to calculate position data based on both angle data and length data, the weight matrix was multiplied to each position data according to the position of the DAR for position estimation [10].

A. POSITION DATA

As mentioned earlier, two position data points are required to estimate the position of the DAR. The position data entail information regarding the location of the anchor ($\boldsymbol{A}_1, \boldsymbol{A}_2$), rope length ($l_1$, l_2), angle of the robot's rotation ψ, angle of the robot and the rope (θ_1, θ_2), and angle of the rope and anchor (θ_3, θ_4). Fig. 3 illustrates a simple model for estimating the position of the robot. The red line denotes the rope, and the black line, the distance between the joints on which the robot is suspended (w).

Based on Fig.3, forward kinematics is applied. The main agent of forward kinematics is from center of joints' position on which the robot is suspended to each anchor's position. These forward kinematics is represented to 4 equations as follow:

$$\boldsymbol{f} = \begin{Bmatrix} A_{1,x} + l_1 \cos\theta_4 + \frac{1}{2} w \cos\psi - x_{A_1} \\ A_{2,x} - l_2 \cos\theta_3 - \frac{1}{2} w \cos\psi - x_{A_2} \\ A_{1,y} - l_1 \sin\theta_4 - \frac{1}{2} w \sin\psi - y_{A_1} \\ A_{2,y} - l_2 \sin\theta_3 - \frac{1}{2} w \sin\psi - y_{A_2} \end{Bmatrix} \quad (1)$$

where x_{A_i}, y_{A_i} are the coordinates of the points on which the robot is suspended from the rope at each anchor ($\boldsymbol{A}_i$) and $\boldsymbol{f}$ is the position error. The two position data points are modified by in turn modifying Eq. (1) based on x_{A_i}, y_{A_i}. Position data based on angle data were calculated by varying the rope length l_i to the angle θ_i of the robot and rope. Subsequently, position data based on length data are the same as that based on the length of the rope (l_1, l_2) as well as that which locates the robot based on the angle ψ of the robot's turn. As with the position data based on the angle data, the angle θ_i of the robot is varied to the rope length l_i in Eq. (1).

B. POSITION ESTIMATION

If the position based on the length or angle of the rope is estimated using two position data points obtained via forward kinematics, the process of weighting the position data is necessary. Position data depend on which data are based on the position of the outer wall. Therefore, to increase position accuracy, the DAR adopted a sensor fusion method, which helps select position data based on length data and angle data by multiplying the weight of the weight matrix [13]. The weight matrix is defined as follows:

$$\text{Minimize } \boldsymbol{f}^T \boldsymbol{\Sigma}_f^{-1} \boldsymbol{f} \quad \text{over } \boldsymbol{x} \quad (2)$$

Eq. (2), the weight matrix is calculated by multiplying the position error $\boldsymbol{f}$ and the weight factor $\boldsymbol{\Sigma}_f^{-1}$ of the position data obtained via forward kinematics. The weight matrix serves as a type of switch and selects reliable data corresponding to the position of the robot between the two position data points; thus, the more accurate are the position data, the better is the performance. However, if the experimental time increases, the position data based on the length data become inaccurate. This is because a greater error in the rope length l_i is accumulated owing to the structural property of the robot; further, a difference is observed in the actual position and data of the robot. To eliminate this error, rope angle-based Kalman filter method is proposed.

III. ROPE ANGLE-BASED KALMAN FILTER METHOD

A. KALMAN FILTER

Kalman filters can be used recursively to solve discrete data linear filtering problems [14]. Because of Kalman filter's recursive use, modelling of the system that is linear is suitable to apply data filtering. The Kalman filter applicable to systems in a linear ideal state is called the linear Kalman filter (LKF) [15]. However, the system does not linear because

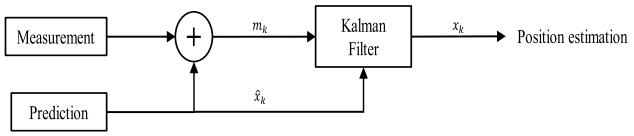

FIGURE 4. Schematic of DAR's Kalman filter method; irrespective of the Kalman filter selected, measurement and prediction data are required.

of various factors such as disturbance in a dynamic state. The Kalman filter, which came out to filter the data of the nonlinear system with disturbance, is called extended Kalman filter (EKF) [16]. However, there are not only linear states and linear states with disturbance in the system. In addition, system defined by nonlinear and modelling itself becomes difficult when a disturbance is added to the nonlinear system. Thus, the Kalman filter, which came out to filter the data of the nonlinear system, is called unscented Kalman filter (UKF) [17], [21]. Although the performances of the three Kalman filters depend on the system modeling, they require measurement data ($\boldsymbol{m}_k$), which are the filtering and prediction data ($\hat{\boldsymbol{x}}_k$) that ensure the filtering standard for filter applications, as shown in Fig. 4. After select two required data, full-fledged filtering could be realized. However, the basic concept of filtering is the same for all three Kalman filters. Data were filtered in five steps. The first step is the prediction step to calculate $\hat{\boldsymbol{x}}_k$ and $\hat{\mathbf{P}}_k$ as follows:

$$\hat{\boldsymbol{x}}_k = \mathbf{A}\boldsymbol{x}_{k-1} \tag{3}$$
$$\hat{\mathbf{P}}_k = \mathbf{A}\mathbf{P}_{k-1}\mathbf{A}^{\mathbf{T}}+\mathbf{Q} \tag{4}$$

where hat denotes the predicted value, and $\mathbf{A}$, the system modeling. Further, the initial values $\boldsymbol{x}_0$, $\mathbf{P}_0$, and noise value $\mathbf{Q}$ must be specified. The second step is to calculate the Kalman gain ($\mathbf{K}_k$) using the values calculated in the first step Eq. (5).

$$\mathbf{K}_k = \hat{\mathbf{P}}_k\mathbf{H}^{\mathbf{T}}(\mathbf{H}\hat{\mathbf{P}}_k\mathbf{H}^{\mathbf{T}} + \mathbf{R})^{-\mathbf{1}} \tag{5}$$
$$\boldsymbol{m}_k = \mathbf{H}\boldsymbol{x}_k \tag{6}$$

where $\mathbf{H}$ represents the relationship between the measurement data ($\boldsymbol{m}_k$) and the status variable, and $\mathbf{R}$ is the noise value Eq. (6). The third step is implemented by calculating the entered measurement data ($\boldsymbol{m}_k$) to estimate the data ($\boldsymbol{x}_k$) Eq. (7).

$$\boldsymbol{x}_k = \hat{\boldsymbol{x}}_k + \mathbf{K}_k\left(\boldsymbol{m}_k - \mathbf{H}\hat{\boldsymbol{x}}_k\right) \tag{7}$$

The fourth step is to obtain the error covariance ($\mathbf{P}_k$), which is the standard for determining the accuracy of the estimation data ($\boldsymbol{x}_k$). The error covariance ($\mathbf{P}_k$) is calculated using Eq. (8).

$$\mathbf{P}_k = \hat{\mathbf{P}}_k - \mathbf{K}_k\mathbf{H}\hat{\mathbf{P}}_k \tag{8}$$

The fifth step is the recursive step. The covariance $\mathbf{P}_k$ obtained in Eq. (8) is substituted in Eq. (4).

B. KALMAN FILTER METHOD ON DAR

To apply the Kalman filter to the DAR, the two aforementioned data, measurement ($\boldsymbol{m}_k$) and prediction data ($\hat{\boldsymbol{x}}_k$), are selected as prerequisites in Fig. 4. First, the data available as measurement data ($\boldsymbol{m}_k$) are the two position data points used by the DAR for rope length-based sensor fusion method. However, position data based on angle data among the two position data points are used as measurement data ($\boldsymbol{m}_k$). This is because the error of the position data, which are based on length data, accumulates. Subsequently, angular acceleration is used as the prediction data ($\hat{\boldsymbol{x}}_k$) and are obtained using the IMU sensor. Once the required main data are determined, the five steps of the Kalman filter are implemented to estimate the position of the DAR. The prediction data ($\hat{\boldsymbol{x}}_k$) are defined as follows:

$$\hat{\boldsymbol{x}}_k = \begin{pmatrix} s_x \\ s_y \end{pmatrix} \tag{9}$$

where s_x, s_y are the coordinates of the robot calculated based on the acceleration values. However, obtaining the prediction data ($\hat{\boldsymbol{x}}_k$) using the acceleration raw data, in turn obtained using the IMU sensor, results in a accumulative error, which is an integral problem. IMU sensor's data accumulative error is similar to nonlinear system with disturbance therefore, DAR uses UKF to overcome this problem. UKF uses the sigma point ($\boldsymbol{\chi}_i$) to surmount dissipation of the data. The sigma point ($\boldsymbol{\chi}_i$) of the acceleration value is selected and the weight (ω_i) is calculated. Then, Eq. (3) is implemented. As such, the DAR uses the characteristics of UKF to employ IMU sensor values as prediction data ($\hat{\boldsymbol{x}}_k$) without cumulative error.

$$\hat{\boldsymbol{x}}_k = \hat{\boldsymbol{x}}_{k-1}\omega_i\boldsymbol{\chi}_i\mathbf{g}\left(\boldsymbol{\chi}_i\right) \tag{10}$$
$$\mathbf{g}\left(\boldsymbol{\chi}_i\right) = (\mathbf{I} + \frac{1}{2}\Delta t^2)\boldsymbol{\chi}_i \tag{11}$$

where Eq. (10) helps calculate the prediction data ($\hat{\boldsymbol{x}}_k$) by the UKF of Eq. (3), $\mathbf{I}$ is identical matrix, Δt is difference between two loop time scales and sigma point ($\boldsymbol{\chi}_i$)'s i represents number of loop. Next, measurement data ($\boldsymbol{m}_k$) is employed as position data based on angle data, as defined previously.

$$\boldsymbol{m}_k = \begin{pmatrix} e_x \\ e_y \end{pmatrix} \tag{12}$$

where e_x, e_y are the x and y values of the position data based on the angle data. Using Eq. (13) and Eq. (14), the error covariance of the prediction data ($\hat{\boldsymbol{x}}_k$) and measurement data ($\boldsymbol{m}_k$) is predicted through unscented transformation (UT) with sigma point ($\boldsymbol{\chi}_i$) and weight (ω_i), obtained using the angular acceleration, in turn obtained using the IMU sensor.

$$\mathbf{P}_{\hat{\boldsymbol{x}}_k} = \mathrm{UT}(\boldsymbol{\chi}_i\omega_i) + \mathbf{Q} \tag{13}$$
$$\mathbf{P}_{m_k} = \mathrm{UT}\boldsymbol{\chi}_i\omega_i + \mathbf{R} \tag{14}$$

$\mathbf{P}$ helps obtain the estimation data ($\boldsymbol{m}_k$) based on gains by calculating the predicted error covariance; $\mathbf{Q}$ and $\mathbf{R}$ denote noise and UT denotes unscented transformation [18]. Through the predicted error covariance, the Kalman

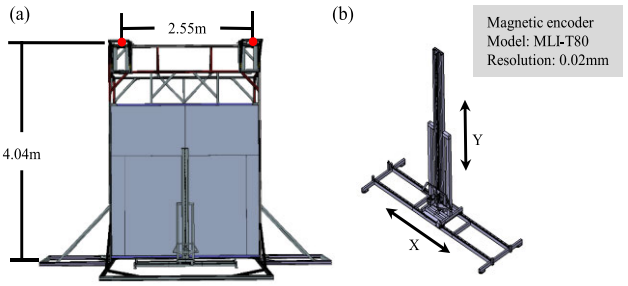

FIGURE 5. Test bench and measurement device: (a) test bench, red points denote rope anchors; (b) measurement device, magnetic encoders are used to measure the DAR's actual position.

gain ($\mathbf{K}_k$) is calculated as shown in Eq. (5) and prediction data ($\hat{\boldsymbol{x}}_k$) is modified based on the Kalman gain ($\mathbf{K}_k$).

$$\mathbf{K}_k = \mathbf{P}_k \mathbf{P}_{m_k}^{-1} \tag{15}$$

$$\mathbf{P}_k = \mathbf{P}_{k-1} \omega_i (\mathbf{g}(\boldsymbol{\chi}_i)\hat{\boldsymbol{x}}_k) \boldsymbol{\chi}_i^{\mathrm{T}} \tag{16}$$

$$\boldsymbol{x}_k = \hat{\boldsymbol{x}}_k + \mathbf{K}_k \boldsymbol{m}_k \tag{17}$$

The final process of the Kalman filter is to obtain the error covariance of the estimation data ($\boldsymbol{m}_k$).

$$\mathbf{P} = \mathbf{P}_{\hat{\boldsymbol{x}}_k} - \mathbf{K}_k \mathbf{P}_{m_k} \mathbf{K}_k^{\mathbf{T}} \tag{18}$$

The error covariance of the obtained measurement data ($\boldsymbol{m}_k$) is calculated using Eq. (13) to recursively filter and continuously estimate the position of the DAR. During all the processes, the Kalman filter method was implemented, which is a new positioning method for the DAR.

IV. EXPERIMENTAL PLANNING

A. TEST BENCH

To compare the performances of the DAR's previous and new position estimation methods, an experiment wherein the robot was practically utilized was conducted. Because the DAR is a façade cleaning robot that hangs on an outer wall via a rope, a test bench with a false wall made by a wood plate that serves as the outer wall of the building is considered along with an anchor that can hang the rope. Fig. 5 (a) is a 3D modeling figure of the test bench with a height of 4 m and whose distance from the anchor ($\boldsymbol{A}_i$) is 2.55 m. At the center of the test bench is a mechanical device, which is used in connection with the DAR. Fig. 5 (b) shows the x- and y-axis coordinates of the robot when it moves over the false wall using the magnetic encoder. The data measured by the measuring device are referred to as the real position data of the robot.

B. EXPERIMENT METHOD AND STANDARD OF COMPARISON

The experiment was commenced by connecting the DAR to the measuring device and then hanging it to the test bench, as shown in Fig. 6 (a). As mentioned earlier, the DAR is a 2-DOF façade cleaning robot and moves in a manner similar to a mobile robot; however, owing to gravity, which does not work in the same direction as that of the mobile robots, a difference in their movements can be observed. This difference means that an evaluation standard for the position estimation accuracy and repeatability of the DAR cannot be set, as can be realized for mobile robots. Therefore, a double ball bar method, which is used in repeatability machines as a basis for evaluation, is employed [19], [20].

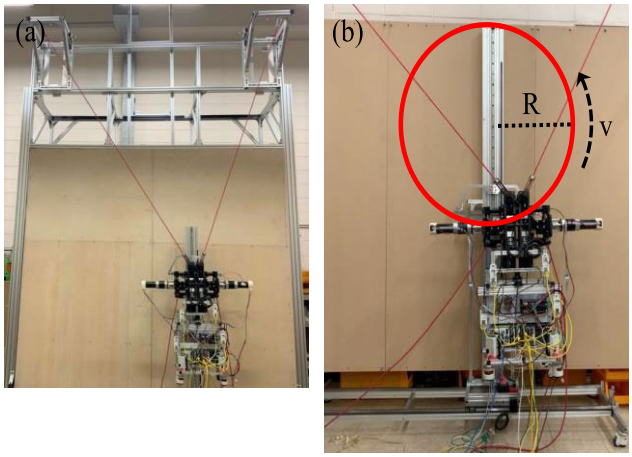

FIGURE 6. DAR's position estimation experiment: (a) hanging DAR from the test bench and (b) implementation of the double ball bar method; R is radius of target movement circle and v is velocity of move.

TABLE 2. Position estimation method comparison experiment.

No	Radius [m]	Velocity [m/s]	Anchor width [m]	Joint offset(w) [m]	# of rotation
1	0.5	0.01	2.55	0.07	4
2	0.5	0.03	2.55	0.07	4

The double ball bar method is employed to assess the accuracy and repeatability of the position or control corresponding to the circular shapes of machines or robots within a certain number of DOFs. This method can be applied to the DAR, such that is can move in a circular motion with a radius of R corresponding to its real position at a speed of v without any control Fig. 6 (b). To verify the accuracy of the position estimation method, position data determined via the sensor fusion method and Kalman filter method were compared with the real position data, and each experiment was conducted four times to obtain information regarding the repeatability. The experiment design is summarized in Table 2.

V. EXPERIMENT RESULTS

The experimental results are plotted in Fig. 7. The figure entails three position data points in total. First, the black data denote the position data obtained using the measurement device (Section 4). Therefore, the measured position is the standard for determining the repeatability and accuracy of other position data. The red data denote the position data obtained via the sensor fusion method, which are the previous

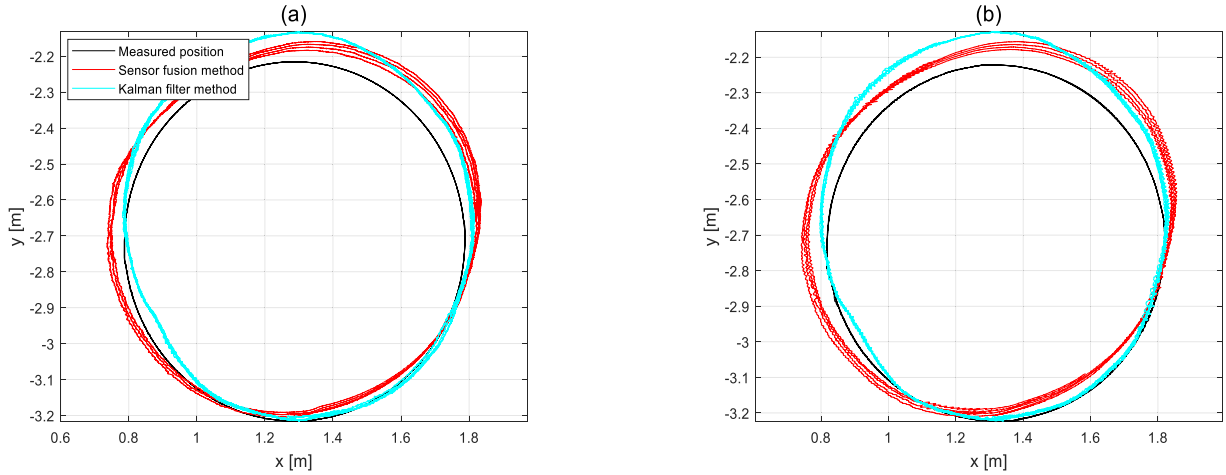

FIGURE 7. Experiment results according to DAR's velocity, each color represent different position data; (a) DAR's velocity = 0.01 m/s; (b) DAR's velocity = 0.03 m/s.

position estimation data of the DAR. Finally, the blue data are the position estimation data obtained using the proposed rope angle-based Kalman filter method. The position data obtained from the experiment were compared in terms of their repeatability and accuracy.

A. REPEATABILITY PERFORMANCE COMPARISON

To estimate the repeatability of the position data, the graphs corresponding to the position data when the DAR was rotated in a circle were created and superimposed. The better is the iteration, the better a graph overlaps with the previous graph. Fig. 7 shows that the graphs obtained for the sensor fusion method, previously used for the DAR position estimation, do not overlap with each other often; this phenomenon is particularly prominent when it ascends or descends toward the highest or lowest point on the y-axis. In contrast, the graphs obtained for the proposed rope angle-based Kalman filter method overlap irrespective of the number of times the circle has been rotated. Quantitative figures were introduced and compared, as summarized in Fig. 8, to more accurately estimate repeatability. During the experiment, the center of the circle was determined corresponding to circle graph and was compared position with the center obtained by previous drawn circle graph. Further, the extent to which the circle overlapped was identified in terms of a root-mean-square error (RMS).

Fig. 8 summarizes that the variation in error is not linear; however, both the sensor fusion and rope angle-based Kalman filter methods exhibit minor errors. The error approximately doubled in the 0.01 m/s experiment and increased by approximately five times in the 0.03 m/s experiment. The results demonstrate that the rope angle-based Kalman filter method was better than the sensor fusion method in terms of repeatability.

B. ACCURACY PERFORMANCE COMPARISON

To estimate the accuracy of position data, the position data obtained via the sensor fusion and rope angle-based Kalman

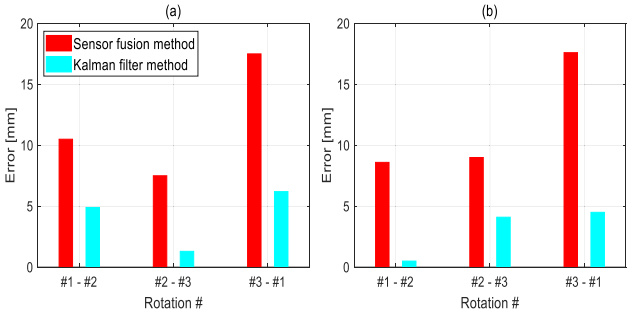

FIGURE 8. Circle center error compare with previous rotation; (a) DAR's velocity = 0.01 m/s; (b) DAR's velocity = 0.03 m/s.

filter methods were compared with the measured position data. The y-axis in the graph in Fig. 9 represents the RMS error. Irrespective of speed, the overall error in the position data obtained via the rope angle-based Kalman filter and sensor fusion methods were similar. However, the two methods exhibit differences as the experiment progresses. In Fig. 9 (a), when the DAR moves at 0.01 m/s, a small error is obtained in the sensor fusion method for 1 to 2 rotations. Fewer errors are observed in the rope angle-based Kalman filter method over time. Unlike Fig. 9 (a), Fig. 9 (b) has fewer position estimation errors in the rope angle-based Kalman filter method in all time zones, irrespective of the number of rotations. The increase in error can evidently be observed in Fig. 10, the error rate. The results confirmed that the rope angle-based Kalman filter method exhibits better accuracy on the x-axis and sensor fusion method on the y-axis. However, the sensor fusion method exhibits one limitation. Fig. 9 shows that the error graph of the rope angle-based Kalman filter method is constant, while that of the sensor fusion method increases. An increase in amplitude means that the accuracy decreases over time. Therefore, if the rope angle-based Kalman filter and sensor fusion methods exhibit similar performance, the more robust rope angle-based Kalman filter method is more accurate.

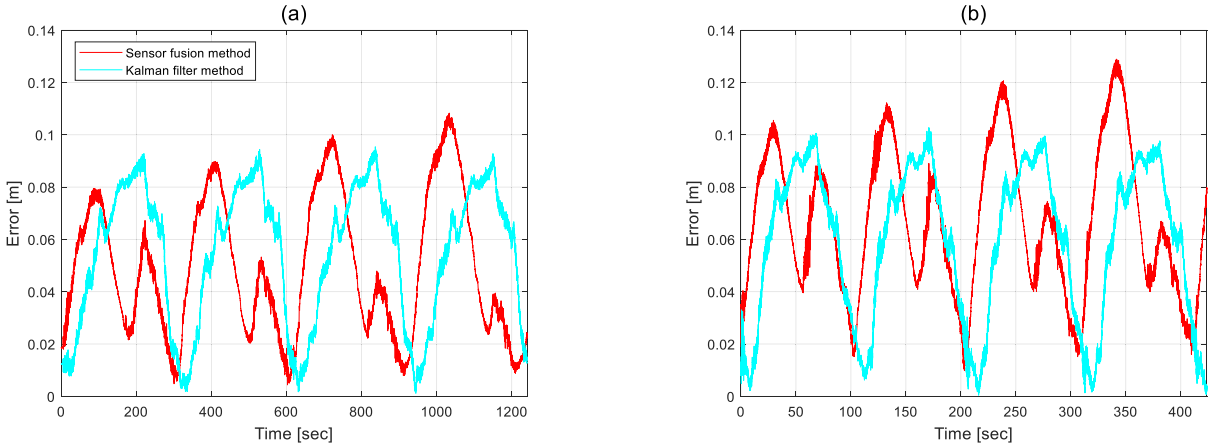

FIGURE 9. Position error relative to a reference, which is measured using a separate device: (a) DAR's velocity = 0.01 m/s; (b) DAR's velocity = 0.03 m/s.

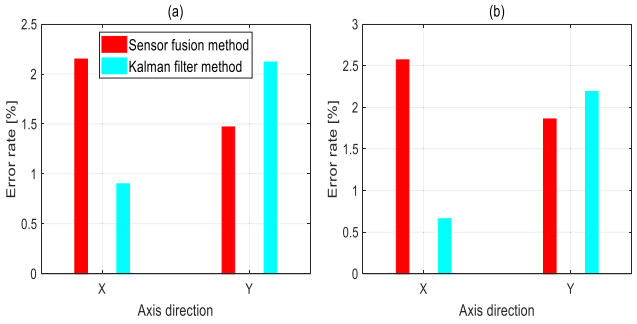

FIGURE 10. Each axis' position estimation error rate; (a) DAR's velocity = 0.01 m/s; (b) DAR's velocity = 0.03 m/s.

VI. CONCLUSION

In this study, a new position estimation method, the Kalman filter method based on rope angle data, was proposed and applied to the DAR. Unlike the previously employed position estimation method, the new position estimation method uses an unscented Kalman filter. Two sets of data, namely, the measurement data and prediction data, are required to apply this unscented Kalman filter. The measurement data did not use position data based on length data; instead, it used position data based on angle data, which rendered the previous position estimation method disadvantageous. The prediction data used the angular acceleration value of the IMU sensor after unscented transformation.

However, the DAR position estimation method was evaluated using the double ball bar method to compare the performance of the new rope angle-based Kalman filter method with that of the sensor fusion method. The double ball bar method evaluates the performance of the machine by making the machine move in a circle. Here, repeatability and accuracy constitute the evaluation standards. Therefore, an experiment involving changing the speed of the DAR and rotating it four times to a circle 0.5 m in radius was also conducted. As a result of the experiment, the rope angle-based Kalman filter method showed better performance in terms of the repeatability of position estimation. Circular overlapping according to rotation occurred more in the rope angle-based Kalman filter method than in the sensor fusion method; moreover, the sensor fusion method gave rise to errors approximately 2–3 times greater than those in the rope angle-based Kalman filter method when the change in the center of the circle position was considered according to each rotation. In terms of the accuracy of position estimations, different degrees of performance were obtained depending on the axis. While the rope angle-based Kalman filter method showed good performance for the x-axis, the sensor fusion method showed good performance for the y-axis. However, as shown in Fig. 8, the amplitude of the sensor fusion method error graph appeared to grow gradually, indicating an increase in error over time. According to the experimental results, the accuracy of the rope angle-based Kalman filter method was also better than that of the sensor fusion method. The rope angle-based Kalman filter method, a new position estimation method for DARs, is applicable to DAR control because it has resulted in improvements in performance in terms of accuracy and repeatability relative to that of the previous method. Overall, it is expected that DAR control with the new position estimation method will become more robust to accumulative length data error.

ACKNOWLEDGMENT

(Myeongjin Choi and Myoungjae Seo contributed equally to this work.)

REFERENCES

[1] T. Seo, Y. Jeon, C. Park, and J. Kim, "Survey on glass and Façade-cleaning robots: Climbing mechanisms, cleaning methods, and applications," *Int. J. Precis. Eng. Manuf.-Green Technol.*, vol. 6, no. 2, pp. 367–376, Apr. 2019.

[2] S. Pro. *Automatic Window and Building Cleaning Robot*. Accessed: Oct. 5, 2020. [Online]. Available: http://www.skyprocy.com /en/products/12-english/36-skypro/

[3] S. Mini, *Automatic Window Cleaning Robot for Mid-Height Building*. Accessed: Oct. 5, 2020. [Online]. Available: https://www.youtube.com/watch?v=dCjB-XcTnSU/.

[4] S. Rajesh, P. Janarthanan, G. Raj, and A. Jaichandran, "Design and optimization of high rise building cleaner," *Int. J. Appl. Eng. Res.*, vol. 13, no. 9, pp. 6881–6885, 2018.
[5] IPC Eagle. *HighRiseTM—HR 202, USA*. Accessed: Oct. 5, 2020. [Online]. Available: http://www.ipcworldwide.com/us/wpcontent/uploads/sites/7/2017/11/High-Rise-Operation-Manual-HR202.pdf
[6] K. Seo, S. Cho, T. Kim, H. S. Kim, and J. Kim, "Design and stability analysis of a novel wall-climbing robotic platform (ROPE RIDE)," *Mech. Mach. Theory*, vol. 70, pp. 189–208, Dec. 2013.
[7] T. Akinfiev, M. Armada, and S. Nabulsi, "Climbing cleaning robot for vertical surfaces," *Ind. Robot. Int. J.*, vol. 36, no. 4, pp. 352–357, Jun. 2009.
[8] *Kiterobotics*. Accessed: Jun. 16, 2020. [Online]. Available: https://www.kiterobotics.com
[9] N. Imaoka, S.-G. Roh, N. Yusuke, and S. Hirose, "SkyScraper-I: Tethered whole windows cleaning robot," in *Proc. IEEE/RSJ Int. Conf. Intell. Robot. Syst.*, Oct. 2010, pp. 5460–5465.
[10] M. Seo, S. Yoo, J. Kim, H. S. Kim, and T. Seo, "Dual ascender robot with position estimation using angle and length sensors," *IEEE Sensors J.*, vol. 20, no. 13, pp. 7422–7432, Jul. 2020, doi: 10.1109/JSEN.2020.2978549.
[11] W. Elmenreich, "An introduction to sensor fusion," Vienna Univ. Technol., Vienna, Austria, Tech. Rep. 47/2001, 2002.
[12] N. Houshangi and F. Azizi, "Accurate mobile robot position determination using unscented Kalman filter," in *Proc. Can. Conf. Electr. Comput. Eng.*, Saskatoon, Sask, 2005, pp. 846–851, doi: 10.1109/CCECE.2005.1557061.
[13] A. Fortin-Cote, P. Cardou, and A. Campeau-Lecours, "Improving cable driven parallel robot accuracy through angular position sensors," in *Proc. IEEE/RSJ Int. Conf. Intell. Robots Syst. (IROS)*, Oct. 2016, pp. 4350–4355.
[14] G. Welch and G. Bishop, "An introduction to the Kalman filter," Dept. Comput. Sci., Univ. North Carolina, NC, USA, Tech. Rep. TR95041, 2000.
[15] R. G. Valenti, I. Dryanovski, and J. Xiao, "A linear Kalman filter for MARG orientation estimation using the algebraic quaternion algorithm," *IEEE Trans. Instrum. Meas.*, vol. 65, no. 2, pp. 467–481, Feb. 2016, doi: 10.1109/TIM.2015.2498998.
[16] J. L. Marins, X. Yun, E. R. Bachmann, R. B. McGhee, and M. J. Zyda, "An extended Kalman filter for quaternion-based orientation estimation using MARG sensors," in *Proc. IEEE/RSJ Int. Conf. Intell. Robot. Syst.*, Maui, HI, USA, 2001, pp. 2003–2011, doi: 10.1109/IROS.2001.976367.
[17] E. A. Wan and R. Van Der Merwe, "The unscented Kalman filter for nonlinear estimation," in *Proc. IEEE Adapt. Syst. Signal Process., Commun., Control Symp.*, Lake Louise, AB, Canada, Dec. 2000, pp. 153–158, doi: 10.1109/ASSPCC.2000.882463.
[18] J. Andrade-Cetto, T. Vidal-Calleja, and A. Sanfeliu, "Unscented transformation of vehicle states in SLAM," in *Proc. IEEE Int. Conf. Robot. Autom.*, Barcelona, Spain, Dec. 2005, pp. 323–328, doi: 10.1109/ROBOT.2005.1570139.
[19] X. Jiang and R. J. Cripps, "A method of testing position independent geometric errors in rotary axes of a five-axis machine tool using a double ball bar," *Int. J. Mach. Tools Manuf.*, vol. 89, pp. 151–158, Feb. 2015.
[20] K.-I. Lee, D.-M. Lee, and S.-H. Yang, "Parametric modeling and estimation of geometric errors for a rotary axis using double ball-bar," *Int. J. Adv. Manuf. Technol.*, vol. 62, nos. 5–8, pp. 741–750, Sep. 2012.
[21] R. Van Der Merwe, "Sigma point Kalman filters for probabilistic inference in dynamic state-space models," Ph.D. dissertation, OGI School Sci. Eng., Oregon Health & Science University, Portland, OR, USA, 2004.
[22] S. J. Julier and J. K. Uhlmann, "Unscented filtering and nonlinear estimation," *Proc. IEEE*, vol. 92, no. 3, pp. 401–422, Mar. 2004.

MYEONGJIN CHOI received the B.S. degree in electronic engineering from Hanyang University, in 2020, where he is currently pursuing the M.S. degree in mechanical engineering. His research interests include the areas of robot mechanism design, control, and optimization.

MYOUNGJAE SEO received the B.S. degree in mechanical engineering from Hanyang University, in 2019, where he is currently pursuing the M.S. degree. His research interests include robot design, control, and optimization.

HWA SOO KIM (Member, IEEE) received the B.S. and Ph.D. degrees from Seoul National University, South Korea, in 2000 and 2006, respectively, both in mechanical engineering. From 2007 to 2008, he was a Postdoctoral Researcher with the Laboratory for Innovations in Sensing, Estimation, and Control, University of Minnesota, Minneapolis, MN, USA. He is currently an Associate Professor with the Department of Mechanical System Engineering, Kyonggi University. His current research interests include design, modeling, and control of various mobile platforms.

TAEWON SEO (Senior Member, IEEE) received the B.S. and Ph.D. degrees from the School of Mechanical and Aerospace Engineering, Seoul National University, South Korea, in 2003 and 2008, respectively. He was a Postdoctoral Researcher with the Nanorobotics Laboratory, Carnegie Mellon University, a Visiting Professor with the Biomimetic Millisystems Lab, University of California, Berkeley, a Visiting Scholar with the University of Michigan, and an Associate Professor with the School of Mechanical Engineering, Yeungnam University, South Korea. He is currently an Associate Professor with the School of Mechanical Engineering, Hanyang University, South Korea. His research interests include robot design, analysis, control, optimization, and planning. He received the Best Paper Award of the IEEE/ASME TRANSACTION ON MECHATRONICS, in 2014. He was an Associate Editor of IEEE ROBOTICS AND AUTOMATION LETTERS. He is a Technical Editor of the IEEE/ASME TRANSACTION ON MECHATRONICS and an Associate Editor of *Intelligent Service Robots*.